yields a p-p scattering length of -7.82 F and effective range of 2.75 F.
[14]K. A. Brueckner, J. L. Gammel, and J. T. Tubis, Phys. Rev. 118, 1095 (1960).
[15]J. S. Levinger and L. M. Simmons, Phys. Rev. 124, 916 (1961).

IMPORTANCE OF THE IMAGINARY TERM IN DISTORTED-WAVE BORN-APPROXIMATION CALCULATIONS OF ^{3}He INELASTIC SCATTERING*

E. R. Flynn

University of California, Los Alamos Scientific Laboratory, Los Alamos, New Mexico

and

R. H. Bassel

Oak Ridge National Laboratory, Oak Ridge, Tennessee

(Received 28 June 1965)

The collective-model and distorted-wave Born-approximation (DWBA) description of the inelastic scattering of nucleons[1] and alpha particles[2] has proven quite successful. In this theory the amplitude for excitation of low-lying collective states takes the form

$$T_{if}=\beta_l\int d\vec{r}\,\chi_f^{(-)*}(\vec{k}_f,\vec{r}_f)\{i^l Y_l^m(\theta',\varphi')\times\left[R_r\frac{dV(r)}{dr}+iR_w\frac{dW(r)}{dr}\right]\chi_i^{(+)}(\vec{k}_i,\vec{r}_i)\}, \quad (1)$$

where the χ's are the distorted waves generated from the optical potential U used to fit the scattering data. Here

$$U(r)=-[V(r)+iW(r)]=-V_0 f(x)-iW_0 f(x');$$
$$f(x)=(1+e^x)^{-1};$$
$$x=(r-R_0)/a;$$
$$x'=(r-R_w)/a_w; \quad (2)$$

and β_l is the usual deformation parameter. In this analysis β_l is the only free parameter, since the optical potential is determined from the elastic scattering and is taken to be the same in both channels.

Equation (1) implies, as usual, that the density distribution is aspherical, and furthermore that the imaginary interaction follows the motion of the nucleus as well as the real interaction. Formally, the imaginary part of the form factor arises in the same manner as the imaginary part of the spherical optical potential.

Most previous analyses of inelastic scattering have made use of the real part of the form factor. Recently the complex form has been applied to inelastic alpha-particle scattering[3] and found to produce somewhat better agreement with the data, but with a small correction to β_l. Similar analyses of nucleon inelastic scattering[4] show a definite improvement over calculations using the real form factor. Here the corrections to β_l are of the order of 10 to 20% for 40-MeV protons. The present Letter presents evidence that the complex form factor in Eq. (1) is necessary to describe the inelastic scattering of ^{3}He ions; indeed, almost all of the cross section arises from the imaginary term.

The experimental data were obtained by scattering 22-MeV ^{3}He ions obtained from the Los Alamos variable-energy cyclotron from thin-foil targets of ^{56,58}Fe and ^{58}Ni. The elastic- and inelastic-scattered particles were detected by means of an $E\times dE/dx$ solid-state counter telescope and displayed on a 400-channel analyzer suitably gated by the multiplier so that only ^{3}He particles were accepted. The angular range of the elastic measurements was from 9° to 150°. The small-angle elastic data were found to be Rutherford, and this allowed normalization of the elastic and inelastic data to obtain accurate absolute cross sections. Only the 2^+ and the 3^- single-phonon states of the three targets were analyzed, these being the most prominent levels found. Analysis of the inelastic states was limited at forward angles because of a low-energy component from the elastic peak due to scattering of the incident beam from collimating slits and the analyzing magnet located in front of the 20-in. scattering chamber.

The elastic data were fitted using the optical-

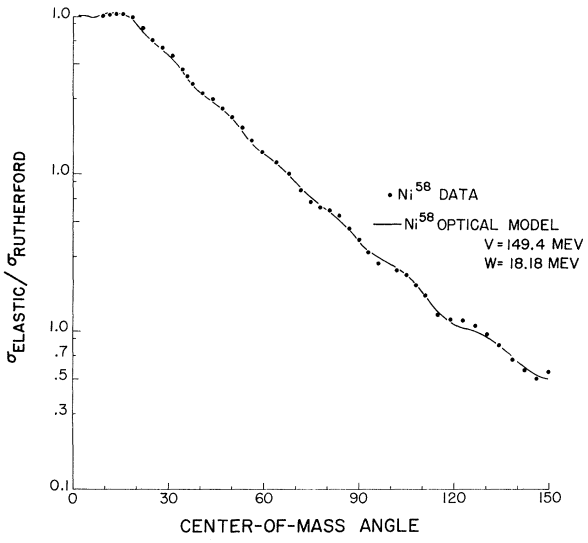

FIG. 1. Optical-model fit to ^{58}Ni elastic data. Parameters used are $V=149.4$ MeV, $W=18.18$ MeV, $r_0=1.08$ F, $r_w=1.63$ F, $a=0.767$ F, and $a_w=0.76$ F.

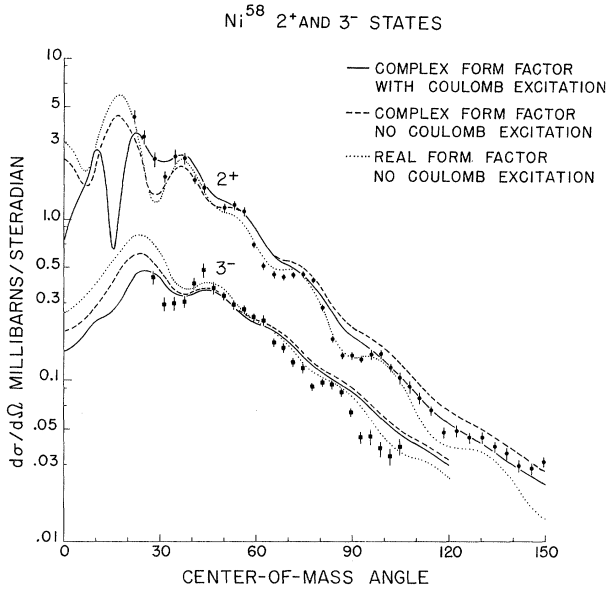

FIG. 2. Comparison of three form factors used in the DWBA calculation. The experimental data are indicated as the points with error bars.

model search code of Perey[5] and also the Oak Ridge code HUNTER.[6] The form of the "nuclear potential" is given in Eq. (2), while the Coulomb interaction was taken to be of the form

$$V_C(r) = 2Ze^2/r, \qquad r \geq R_c,$$

$$= (Ze^2/R_c^2)(3-r^2/R_c^2), \qquad r \leq R_c.$$

The elastic-scattering data and the optical-model fits are shown in Fig. 1 for ^{58}Ni. Although several sets of parameters were found which fit the elastic data equally well, the inelastic calculations were insensitive to which set was used provided the elastic data were well fitted. Here we confine our attention to a parameter set that is consistent with the parameters found by Armstrong, Blair, and Bassel,[7] which describe ^{3}He elastic scattering from a range of targets. The parameters for ^{58}Ni are listed in Fig. 1.

In Fig. 2 are shown three separate calculations for the 2^+ and 3^- states of ^{58}Ni as given by the DWBA code JULIE.[6] These include the cases where (1) only the real part of U was considered, or a real form factor (RFF); (2) the entire U was used, or complex form factor (CFF); and (3) the complex form factor was used, but corrected for Coulomb excitation. In Table I are shown the values of β_l extracted from comparing the calculated distribution with the data. Also in this table are the values obtained for ^{56,58}Fe. The β_l found from these experiments are compared with previously reported values. It is obvious from this table that the imaginary part of the potential contributes almost all of the scattering cross section, in contrast to what is found in alpha-particle and nucleon scattering. It has been suggested[8] that βR rather than β should be used for comparing various measurements. In this case the interaction radius R is not uniquely

Table I. Values of deformation parameter for ^{56,58}Fe and ^{58}Ni for the 2^+ (β_2) and 3^- (β_3) states. RFF is the real form factor, CFF the complex form factor, and CE the Coulomb excitation correction.

		RFF	CFF	CFF and CE	Reported values
^{56}Fe	β_2	0.48	0.22	0.19	0.19→0.27
	$\beta_2 R_i$	2.86	1.29	1.12	0.87→1.24
	β_3	0.24	0.11	0.10	0.10→0.11
	$\beta_3 R_i$	1.41	0.63	0.60	0.46→0.51
^{58}Fe	β_2	0.62	0.22	0.18	0.17→0.25
	$\beta_2 R_i$	3.77	1.31	1.09	0.79→1.16
	β_3	0.23	0.082	0.080	0.08
	$\beta_3 R_i$	1.36	0.50	0.48	0.37
^{58}Ni	β_2	0.58	0.18	0.15	0.15→0.21
	$\beta_2 R_i$	3.63	1.12	0.95	0.93→1.01
	β_3	0.32	0.10	0.10	0.13→0.21
	$\beta_3 R_i$	2.04	0.66	0.65	0.86

defined, but βR_W compares well with previously reported values, as can be seen in Table I, again indicating the dominance of the imaginary form factor.

It should be noted that at large angles the complex form-factor predictions have lost most of their structure, while the shape of the real-form prediction is in rough agreement with the data. This suggests that the distorted-wave prescription is suppressing important contributions from the interior—due most probably to the large strength of the imaginary potential needed to fit the elastic scattering.

It is well known that the strong quadrupole state accounts for some 30% of the imaginary well depth W for nucleons, and it is reasonable to expect a comparable or large effect in this case. We are presently investigating the inclusion of the 2^+ state in "coupled equations,"[9] and these results, as well as a more complete discussion of the data and theoretical analysis, will be presented in due course.

We are grateful to L. Rosen, R. M. Drisko, G. R. Satchler, and T. Tamura for valuable discussions.

*Work performed under the auspices of the U. S. Atomic Energy Commission.

[1]B. Buck, Phys. Rev. 130, 712 (1963); G. R. Satchler, R. H. Bassel, and R. M. Drisko, Phys. Letters 5, 256 (1963).

[2]R. H. Bassel, G. R. Satchler, R. M. Drisko, and E. Rost, Phys. Rev. 128, 2693 (1962).

[3]H. W. Broek, J. L. Yntema, B. Buck, and G. R. Satchler, to be published.

[4]M. P. Fricke and G. R. Satchler, Phys. Rev. 139, B567 (1965); K. Yagi, H. Egiri, M. Furukawa, Y. Ishizaki, M. Koike, K. Matsuda, Y. Nakajima, I. Nonaka, Y. Saji, E. Tanaka, and G. R. Satchler, Phys. Letters 10, 186 (1964).

[5]F. G. Perey, Phys. Rev. 131, 745 (1963).

[6]R. M. Drisko, unpublished.

[7]D. D. Armstrong, A. G. Blair, and R. H. Bassel, to be published.

[8]J. S. Blair, Conference on Direct Interactions and Nuclear Reaction Mechanisms, Padua, Italy, 1962, edited by E. Clementel and C. Villi (Gordon and Breach Publishers, Inc., New York, 1963).

[9]See, e.g., reference 1, and T. Tamura, to be published.

CONTINUUM RESONANCES IN $He^4(p,p')He^{4*}$ †

Lawrence E. Williams

University of Minnesota, Minneapolis, Minnesota

(Received 18 June 1965)

Two and possibly three resonances have been seen in the inelastic-proton continuum resulting from 40-MeV proton bombardment of a NTP He^4 gas target. The incident proton energy, E_p, was defined to within ±60 keV by an edge-focused 60° wedge magnet. The gas target was kept in continuous flow to preclude chamber contamination due to (1) out gassing, or (2) residual air left in the vessel during gas transfer. Background spectra with air as the target revealed no proton-continuum structure in the region of excitation, $19 \leq E^* \leq 24$ MeV, observed in He^4. Throughout the angular range of the experiment, $15° \leq \theta_{lab} \leq 90°$, inelastic protons were detected by an array of 32 solid-state passing detectors mounted in the focal plane of a 180° double-focusing magnetic spectrometer. Neglecting the logarithmic term in the energy-loss formula, it is easily shown that the pulse height of a passing particle at a given magnetic field and fixed radius of curvature is proportional to its mass squared. Thus d, T, He^3, and He^4 particles were discriminated against after the expected He^4 inelastic-proton pulse height was determined from an $H(p,p)H$ scattering at an appropriate angle. Hydrogen elastic scattering was also used to energy-calibrate the spectrometer magnetic field. Thus, with a knowledge of incident beam energy, target purity, and detected particle type and energy, an absolute determination of the resonance Q values could be obtained. The lowest excitation, and relatively narrow resonance (I) occur at 0.64 ±0.14 MeV above the continuum onset due to the reaction $(He^4 + p \rightarrow 2p + T)$. The second and broader resonance occurs at 2.18 ± 0.14 MeV above the $p + T$ breakup point. From Figs. 1 and 2, which show $\partial^2\sigma/\partial\omega\,\partial p$ versus spectrometer field (B_0) at $\theta = 25°$ and 52°, respectively, it is seen that both peaks are superimposed upon a background consisting of phase-space continuum and an additional experimental "flat" continuum which is observed at B_0 values above